Mineralogy and Petrology (2002) 74: 1–24

Mineralogy and Petrology



# Chemical evolution and petrogenetic implications of loparite in the layered, agpaitic Lovozero complex, Kola Peninsula, Russia

**L. N. Kogarko**[1], **C. T. Williams**[2], and **A. R. Woolley**[2]

[1] Vernadsky Institute, Moscow, Russia
[2] Department of Mineralogy, Natural History Museum, London, United Kingdom

With 8 Figures

Received November 6, 2000;
revised version accepted January 18, 2001

**Summary**

Lovozero, the largest of the world's layered peralkaline intrusions, includes gigantic deposits of Nb + REE-loparite ore. Loparite, $(Na,Ce,Ca)_2(Ti,Nb)_2O_6$, became a cumulus phase after crystallisation of about 35% of the 'Differentiated Complex', and its compositional evolution has been investigated through a 2.35 km section of the intrusion. The composition of the cumulus loparite changes systematically upwards through the intrusion with an increase in Na, Sr, Nb and Th and decrease in REE and Ti. This main trend of loparite evolution records differentiation of the peralkaline magma through crystallisation of 1600 m of the intrusion. The formation of the loparite ores was the result of several factors including the chemical evolution of the highly alkaline magma and mechanical accumulation of loparite at the base of a convecting unit. At later stages of evolution, when concentrations of alkalis and volatiles reached very high levels, loparite reacted with the residual melt to form a variety of minerals including baryto-lamprophyllite, lomonosovite, steenstrupine-(Ce), vuonnemite, nordite, nenadkevichite, REE, Sr-rich apatite, vitusite-(Ce), mosandrite, monazite-(Ce), cerite and Ba, Si-rich belovite. The absence of loparite ore in the ''Eudialyte complex'' is likely to be a result of the wide crystallisation field of lamprophyllite, which here became a cumulus phase.

## Introduction

The most alkaline igneous systems are represented by more than 70 occurrences of agpaitic nepheline syenite including the large intrusions of Lovozero and Khibina (Kola Peninsula, Russia), Ilímaussaq (Greenland), Pilanesberg (South Africa) and Poços de Caldas (Brazil). These rocks are extremely enriched in volatiles (F, Cl, S)

and rare elements, as well as alkalis. Agpaitic rocks are peralkaline nepheline syenites characterised by complex Zr and Ti minerals such as eudialyte and mosandrite rather than simple minerals such as zircon and ilmenite (*Le Maitre*, 1989, p. 41). The high alkalinity is the reason, owing to the changing of the melt structure, for the presence in these rocks of a broad range of minerals such as chemically complex sodium-rich zirconium-, niobium- and titanium-bearing silicates containing abundant volatile components. It has been demonstrated (*Kogarko*, 1990) that the high alkalinity of agpaitic magmas inhibits the separation of volatile and rare metals (i.e. rare earth elements, Zr, Hf, Nb, Ta, Th, U, Sr, Ba) into the fluid phase, while the magmatic system remains closed with regard to these components.

Loparite, with the general formula $(Na,Ce,Ca)_2(Ti,Nb)_2O_6$, is a member of the perovskite structural group (*Mitchell*, 1996). It is an accessory mineral in a number of occurrences of agpaitic rocks but is only present in significant amounts in the Lovozero complex, where it is concentrated in some layers up to 25% by volume (*Gerasimovsky* et al., 1966), and forms the world's largest known (Nb + REE) deposit. Loparite mineralisation is closely connected with the igneous layering at Lovozero (*Vorob'eva*, 1938; *Gerasimovsky* and *Kostyleva*, 1937; *Smirnov*, 1976) and one of the principal aims of the present study of the mineralogy of Lovozero was to investigate the compositional evolution of the loparite during crystallisation in this highly alkaline igneous environment. It is generally assumed that in giant intrusions magmatic sedimentation leads to crystal accumulation and, in closed systems, element concentrations in the melt will change, mostly depending on the partition coefficients of the crystallising phases. This process must certainly influence loparite composition (as a cumulus phase) through the vertical section of Lovozero and will be expressed as cryptic variation in the loparite.

Following on from earlier studies by *Kogarko* et al. (1996) and *Mitchell* and *Chakhmouradian* (1996), we provide new data to demonstrate clearly the existence of cryptic variation in the loparite through most of the Lovozero intrusion, which constitutes strong evidence of the magmatic origin of the loparite deposits, in contrast to the suggestion of some authors (*Eliseev* and *Fedorov*, 1953; *Ifantopulo* and *Osokin*, 1979) that the loparite ore is of metasomatic origin.

During the very late evolution of the agpaitic magma, when concentrations of volatile components and alkalis reached very high levels, hyperagpaitic minerals (*Khomyakov*, 1995) might be expected to form. Loparite becomes unstable and reacts with residual melt to form a wide range of interstitial minerals.

This study forms part of a continuing research programme to re-examine the mineralogy and petrology of the Lovozero layered complex employing modern microanalytical techniques.

## Geological setting

The Lovozero complex is located in the central part of the Kola Peninsula (Fig. 1). The massif is rectangular in plan, has an area of 650 $km^2$ and lies in a northwesterly striking tectonic zone within which a sunken, east-west-trending belt of Palaeozoic rocks has been preserved. Immediately west of Lovozero is the even larger Khibina alkaline massif (*Kogarko* et al., 1995).

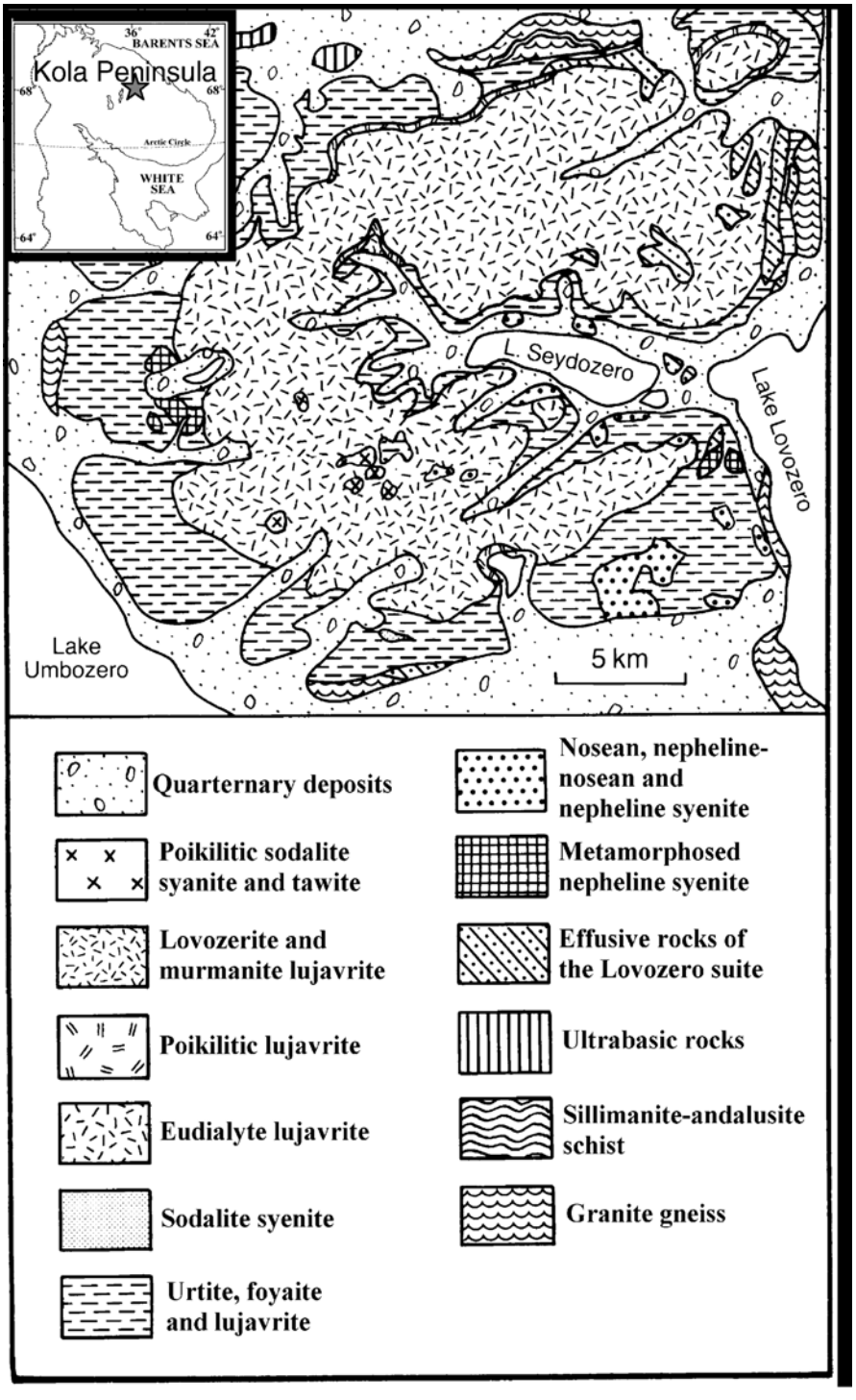


Fig. 1. Geological map of the Lovozero complex with inset showing location of Lovozero (star) within the Kola Peninsula

The Lovozero intrusive complex is emplaced in Archaean granite gneisses and has the form of a lopolith with a broad base (*Gerasimovsky* et al., 1966). According to *Arzamastsev* et al. (1998) the gigantic magma chamber of Lovozero is trough-shaped with a feeding channel situated in the south-western part of the intrusion. The geophysical work of *Shablinskiy* (1963) indicates that the alkaline rocks can be traced to a depth of more than seven kilometres, but their lower limit has not been determined.

The rocks of the Lovozero complex comprise four units, formed in four distinct intrusive phases. The rocks of Phase I occupy only about 5% of the total area, but it is possible that the extent of these rocks increases with depth. The rocks of Phase II comprise the main area (77%) and those of Phase III a lesser amount (18%). Rare dykes of Phase IV are volumetrically insignificant (0.01%). Recently, on the basis of new geological and geophysical data, it has been suggested that ultrabasic alkaline magma was intruded, which comprised about 25% of the total volume of Lovozero, before the first manifestation of nepheline syenite (*Arzamastsev* et al., 1998).

The oldest intrusive formations (Phase I) are even-grained nepheline syenites, nepheline-nosean syenites, poikilitic nosean syenites and metamorphosed nepheline syenites. The latter occur as rare xenoliths and display evidence of alkaline metasomatism and recrystallisation. Feldspar and nepheline replace the primary mineral assemblage and develop granoblastic accumulations, and late aegirine forms fibrous aggregates. The origin of these rocks is not clear, but they are likely to have formed as a result of shearing from emplacement of later intrusions (*Gerasimovsky* et al., 1996, pp 38–40). Amongst this assemblage there are suites of hypabyssal character (nepheline-syenite porphyries set in a fine-grained groundmass containing nepheline, feldspar, clinopyroxene and accessory minerals), seen only as xenoliths. The rocks of Phase I, occurring in their original position, are located in the marginal parts of the complex, and were encountered *in situ* by drilling into the lowermost part of the intrusion. Abundant xenoliths of Phase I rocks are found throughout the complex in rocks of later phases. These rocks are miaskitic (coefficient of agpaicity $< 1$) and do not contain typical agpaitic minerals such as loparite. The main rock-forming minerals of Phase 1 are K–Na feldspar, nepheline, nosean, aegirine-diopside and magnesioriebeckite, with typical accessory minerals represented by ilmenite, titanite, apatite and låvenite.

Phase II comprises a strongly differentiated complex of urtite, foyaite and lujavrite, and is also referred to as the ''Differentiated Complex''. Phase II consists of a layered sequence with, as seen in vertical sections, a regular alternation of layers of urtite, juvite, foyaite and aegirine and amphibole lujavrite (for descriptions of these rock types see *Vlasov* et al., 1966) which range in thickness from a few centimetres to hundreds of metres. The stratigraphic order of the rock types is the same in the various parts of the massif, and the inward dips of the layers are at low angles and vary little between the margins and the centre of the complex. Among the lujavrites there are lens-like bodies of poikilitic sodalite syenite. The rocks of Phase II are more alkaline than Phase I (agpaicity $> 1$). The main rock-forming minerals are nepheline, microcline, sodalite, aegirine and arfvedsonite. The accessory phases are typically enriched in elements such as Sr, Zr, Nb, Ba and REE, and include eudialyte, lomonosovite, murmanite, lamprophyllite, villiaumite, loparite, lorenzenite, apatite and titanite. (The formulae of some of the ''exotic'' minerals

Table 1. *Mineral formulae for the "exotic" mineral phases*

| Mineral name | Formula |
|---|---|
| Barytolamprophyllite | $(Na,K)_2(Ba,Ca,Sr)_2(Ti,Fe)_3(SiO_4)_4(O,OH)_2$ |
| Belovite-(Ce) | $Sr_3Na(Ce,La)(PO_4)_3(F,OH)$ |
| Cerite-(Ce) | $Ce_9^{3+}Fe^{3+}(SiO_4)_6[(SiO_3)(OH)](OH)_3$ |
| Eudialyte | $Na_{15}Ca_6(Fe^{2+},Mn^{2+})_3Zr_3(Si,Nb)(Si_{25}O_{73})(O,OH,H_2O)_3(Cl,OH)_2$ |
| Lamprophyllite | $Na_2(Sr,Ba)_2Ti_3(SiO_4)_4(OH,F)_2$ |
| Lomonosovite | $Na_2Ti_2Si_2O_9.Na_3PO_4$ |
| Loparite-(Ce) | $(Ce,Na,Ca)(Ti,Nb)O_3$ |
| Lorenzenite | $Na_2Ti_2Si_2O_9$ |
| Mosandrite* | $(Ca,Na,Ce)_{12}(Ti,Zr)_2Si_7O_{31}H_6F_4$ |
| Murmanite | $Na_2(Ti,Nb)_2Si_2O_9.n\ H_2O$ |
| Nenadkevichite | $(Na,Ca,K)(Nb,Ti)Si_2O_6(O,OH).2H_2O$ |
| Nordite-(Ce) | $Na_3SrCeZnSi_6O_{17}$ |
| Steenstrupine-(Ce) | $Na_{14}Ce_6Mn^{2+}Mn^{3+}Fe_2^{2+}(Zr,Th)(Si_6O_{18})_2(PO_4)_7.3H_2O$ |
| Villiaumite | NaF |
| Vitusite-(Ce) | $Na_3(Ce,La,Nd)(PO_4)_2$ |
| Vuonnemite | $Na_5Nb_3Ti(Si_2O_7)_3O_2F_2.2Na_3PO_4$ |

*from *Clark* (1993); all others from *Mandarino* (1999)

discussed in this study are given in Table 1.) In the Differentiated Complex, loparite can be locally concentrated in "ore layers" where it occurs mostly as a cumulus mineral at modal proportions $> 1$–$2$ vol.%, and where the stratigraphical position of the layers are well-constrained.

The rocks of intrusive Phase III comprise a suite of eudialyte lujavrites which cut, and overlie, the upper part of the rocks of Phase II (Phase III is known as the "Eudialyte Complex"). The plane of contact between rocks of Phases II and III dips towards the centre of the complex with the angle increasing from the margins towards the centre. The rocks of Phase III form the summits of the mountains of the Lovozero Massif, and the thickness of this suite reaches 450 m but, because of erosion, decreases from northwest to southeast. The rocks of Phase III include leucocratic, mesocratic and melanocratic eudialyte lujavrites, eudialyte foyaite and juvite and a coarser layering is developed than in the rocks of Phase II. At the boundary with the rocks of Phase II there are bodies of porphyritic lujavrite, which are probably partly-quenched varieties of eudialyte lujavrite. Individual veins of porphyritic lujavrite, which are late derivatives of Phase III, up to several kilometres long and 50 m wide, cut the rocks of Phases I and II. Poikilitic sodalite syenite and tawite (sodalitite with some aegirine and minor nepheline, alkali feldspar and eudialyte) are found in the form of equidimensional, sharply defined bodies (generally some 10 s of metres across) amongst the rocks of Phase III and II. The main rock-forming minerals of Phase III are nepheline, microcline, aegirine, eudialyte, lamprophyllite and arfvedsonite. Eudialyte in this complex is euhedral, which is the principal difference from that in the lujavrite of Phase II. The common accessory minerals are lomonosovite-murmanite, loparite, lovozerite, pyrochlore and sodalite.

The rocks of intrusive Phase IV consist of rare dykes of alkaline lamprophyres (monchiquite, fourchite, tinguaite, etc.) which cut all the older alkaline rocks and the surrounding granite gneisses.

## Source of specimens

In spite of extensive drilling the exact form of the Lovozero complex is not known. In Fig. 2 a generalised section (not to scale) is presented to illustrate the broad relationships of the principal units and the approximate positions of the drill holes from which the specimens on which this study are based were collected. It should be noted that drill holes 144 and 178 penetrated most of Phase III. Drill hole 272B is confined to the lower part of Phase II, the lowest part of which was sampled by drill holes 469, 904 and 905. The upper part of Phase II is mostly covered by drill hole 521. The samples from the middle zone were collected from surface outcrop.

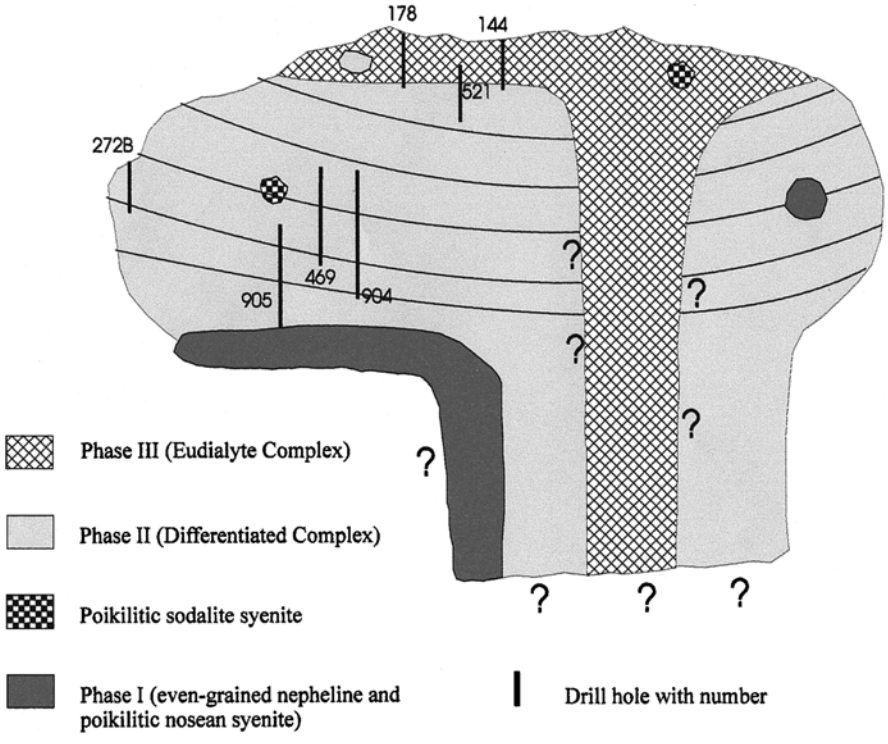


Fig. 2. Schematic cross-section of the Lovozero intrusion, with vertical scale approximately five times horizontal scale, to show the general relationships of the principal rock types and the relative positions, and numbers, of the drill holes sampled during this study. The layering of the Differentiated Complex is illustrated in a simplified form. Bodies of poikilitic sodalite syenite and poikilitic nosean syenite are shown schematically to indicate their relative positions. The geophysical information is not sufficient to constrain the form of the deeper levels of the intrusion. Note that the upper and lower parts of the Differentiated Complex have been extensively drilled but that a section in the lower upper part is unrepresented

The samples that were collected from the surface could not be correlated very accurately with the stratigraphy determined from the various drill cores. Numerous samples of loparite were also collected from mines and from many shorter cores from holes drilled into individual units. In total, 673 microprobe analyses of loparite from 136 samples spanning 2.6 km were obtained from the Lovozero massif. (The full data set can be obtained from any one of the authors on request.)

## Distribution of loparite

The composition of loparite has been studied principally in Phases II and III of the Lovozero massif (Table 2). Although it is very rare in pegmatites, loparites in three pegmatite samples from Phase II and one sample from a Khibina pegmatite were also studied. According to our investigations, and the data of *Gerasimovsky* et al. (1966), loparite is absent from the rocks of Phase I and it is extremely rare in late veins of porphyritic eudialyte lujavrite. In the upper zone of Phase II loparite is particularly enriched in thin seams of malignite (nepheline, minor feldspar and aegirine) where its concentration may reach about 25% by volume. Usually, however, the loparite is concentrated (up to 2–3 vol.%) in urtite and juvite layers and in the upper part of lujavrite layers.

In Phase III, loparite is commonly an accessory mineral and its concentration is about 0.2 vol.%. Only one layer of eudialyte-bearing juvite contains as much as 2–3 vol.% of loparite.

In the rocks of Phases II and III loparite forms two distinctive morphologies:

(a) Well-defined idiomorphic cubes, octahedra (Fig. 3) or twins on the fluorite law. Commonly this loparite is associated with aggregates of aegirine and amphibole. Such crystals vary in diameter from 0.1 to several millimetres. In urtite seams, particularly where loparite concentrations are high, loparite grains have a very uniform size indicating a high level of sorting had occurred, similar to that for the Khibina apatite deposit (*Kogarko* and *Khopaev*, 1987). There is some indication of sorting by size of loparite grains in the urtite seams, and is particularly noticeable when the loparite concentration is high. This loparite we term as "cumulus" loparite.
(b) Interstitial, anhedral crystals. Loparite commonly develops in the interstices of cumulus minerals, mainly nepheline and feldspar, as irregular, poikilitic crystals (Fig. 4). The size of these crystals is variable ranging from tens of microns to millimetre-sized. This morphological variety crystallised at a late stage, and from trapped interstitial melt.

In the rocks of the lowest part of Phase II (1,500–2,350 m below upper contact of Phase II) only interstitial, anhedral loparite occurs (Fig. 4, type (b)). It should be emphasised that in this part of the intrusion, interstitial loparite is associated with titanite, ilmenite and apatite, all as cumulus phases, and the layering is less marked. Some urtite layers in this part of the intrusion have been found that contain 3–5 vol.% of cumulus titanite. In the middle and upper zone of the Differentiated complex, i.e. from 0–1500 m below the contact with the Eudialyte complex, the majority of loparite occurs as a cumulus mineral (type (a)), but a minor proportion exists also as an interstitial phase (i.e. type (b)).

Table 2. *Representative microprobe analyses of loparite*

| Analysis No. | 1 | 2 | 3 | 4 | 5 | 6 | 7 | 8 | 9 | 10 | 11 | 12 | 13 | 14 | 15 |
|---|---|---|---|---|---|---|---|---|---|---|---|---|---|---|---|
| Depth (m) | −1267 | −1331 | −1143 | −1140 | −1136 | −830 | −305 | 50 | 150 | 197 | −2045 | −181 | 175 | | |
| Rock type | Poikilitic sodalite svenite | Juvite | Juvite | Foyaite | Lujavrite | Loparite-apatite ore | Loparite urtite | Loparite juvite | Eudialyte lujavrite | Eudialyte lujavrite | Lujavrite | Foyalite | Eudialyte lujavrite | Pegmatite | Pegmatite |
| Location | Phase II | Phase II | Phase II | Phase II | Phase II | Phase II | Phase II | Phase III | Phase III | Phase III | Phase II | Phase II | Phase III | Khibina | Lovozero |
| Form | Cum | Cum | Cum | Cum | Cum | Cum | Cum | Cum | Cum | Cum | Inter | Inter | Inter | Pegmatite | Pegmatite |
| $Na_2O$ | 8.48 | 8.73 | 8.65 | 8.62 | 8.59 | 8.42 | 8.71 | 8.86 | 9.62 | 9.39 | 9.59 | 11.35 | 15.89 | 10.15 | 8.36 |
| CaO | 4.94 | 4.75 | 3.94 | 4.06 | 4.32 | 4.48 | 4.66 | 4.13 | 2.98 | 2.97 | 3.77 | 2.76 | 0.64 | 2.02 | 4.62 |
| $TiO_2$ | 41.36 | 40.90 | 40.72 | 40.47 | 40.48 | 40.42 | 39.35 | 38.61 | 35.19 | 36.53 | 36.35 | 33.18 | 11.41 | 35.10 | 39.84 |
| FeO | 0.54 | 0.29 | 0.53 | 0.35 | 0.44 | 0.27 | 0.35 | 0.12 | 0.09 | <0.05 | <0.05 | <0.05 | 0.24 | 0.06 | 0.27 |
| SrO | 1.14 | 1.17 | 1.45 | 1.40 | 1.54 | 2.40 | 3.64 | 4.46 | 5.24 | 4.69 | 3.05 | 2.06 | 3.08 | 1.88 | 3.69 |
| $Y_2O_3$ | 0.02 | <0.02 | <0.02 | 0.02 | <0.02 | <0.02 | <0.02 | <0.02 | <0.02 | <0.02 | <0.02 | <0.02 | <0.02 | <0.02 | <0.02 |
| $Nb_2O_5$ | 6.92 | 6.61 | 7.50 | 7.58 | 7.10 | 7.67 | 8.73 | 10.56 | 16.56 | 13.05 | 15.06 | 21.88 | 57.83 | 16.95 | 9.16 |
| BaO | 0.10 | 0.39 | 0.07 | 0.04 | 0.05 | 0.20 | 0.10 | 0.24 | 0.31 | 0.13 | <0.05 | <0.05 | <0.05 | 0.53 | 0.56 |
| $La_2O_3$ | 9.03 | 9.10 | 9.51 | 9.14 | 9.40 | 8.95 | 8.36 | 8.32 | 8.06 | 8.12 | 7.41 | 7.72 | 2.95 | 12.57 | 8.52 |
| $Ce_2O_3$ | 19.44 | 19.65 | 19.73 | 19.21 | 19.50 | 18.34 | 17.50 | 16.43 | 14.69 | 15.55 | 14.76 | 14.60 | 3.86 | 16.17 | 16.66 |
| $Pr_2O_3$ | 1.62 | 1.76 | 1.64 | 1.67 | 1.50 | 1.64 | 1.62 | 1.57 | 1.47 | 1.39 | 1.28 | 1.02 | 0.19 | 0.85 | 1.48 |
| $Nd_2O_3$ | 4.28 | 4.53 | 4.23 | 4.37 | 3.99 | 3.99 | 4.44 | 4.41 | 3.57 | 3.93 | 4.55 | 2.63 | 0.43 | 1.46 | 4.20 |
| $Sm_2O_3$ | 0.17 | 0.24 | <0.15 | 0.24 | <0.15 | 0.30 | 0.16 | 0.25 | 0.21 | <0.15 | 0.36 | <0.15 | <0.15 | <0.15 | 0.24 |
| $Ta_2O_5$ | 0.69 | 0.51 | 1.04 | 0.82 | 0.60 | 0.64 | 0.71 | 0.72 | 1.15 | 0.95 | 0.92 | 1.19 | 0.89 | 0.44 | 0.67 |
| $ThO_2$ | 0.53 | 0.44 | 0.52 | 0.79 | 0.42 | 0.63 | 0.86 | 0.84 | 0.65 | 0.78 | 1.16 | 1.33 | 0.47 | 1.11 | 0.86 |
| $UO_2$ | 0.10 | 0.25 | <0.1 | <0.1 | <0.1 | <0.1 | 0.10 | 0.10 | 0.10 | <0.1 | <0.1 | 0.21 | 0.25 | 0.13 | <0.1 |
| Total | 99.32 | 99.33 | 99.53 | 98.78 | 97.93 | 98.35 | 99.28 | 99.62 | 99.89 | 97.48 | 98.26 | 99.93 | 98.13 | 99.50 | 99.19 |
| $(Y+REE)_2O_3$ | 34.54 | 35.29 | 35.11 | 34.65 | 34.39 | 33.22 | 32.08 | 30.98 | 28.00 | 28.99 | 28.37 | 25.97 | 7.42 | 31.05 | 31.10 |
| cations calculated to 3 oxygens | | | | | | | | | | | | | | | |
| Ca | 0.152 | 0.147 | 0.122 | 0.126 | 0.135 | 0.140 | 0.145 | 0.128 | 0.093 | 0.094 | 0.192 | 0.084 | 0.019 | 0.143 | 0.140 |
| Sr | 0.019 | 0.020 | 0.024 | 0.024 | 0.026 | 0.040 | 0.061 | 0.075 | 0.088 | 0.080 | 0.042 | 0.034 | 0.051 | 0.061 | 0.061 |
| Ba | 0.001 | 0.004 | 0.001 | 0.000 | 0.001 | 0.002 | 0.001 | 0.003 | 0.004 | 0.002 | 0.000 | 0.000 | 0.001 | 0.005 | 0.006 |
| Na | 0.472 | 0.490 | 0.484 | 0.486 | 0.486 | 0.475 | 0.489 | 0.497 | 0.525 | 0.537 | 0.498 | 0.625 | 0.874 | 0.488 | 0.469 |
| Y | 0.000 | 0.000 | 0.000 | 0.000 | 0.000 | 0.000 | 0.000 | 0.000 | 0.000 | 0.000 | 0.000 | 0.000 | 0.000 | 0.000 | 0.000 |
| La | 0.096 | 0.097 | 0.101 | 0.098 | 0.101 | 0.096 | 0.089 | 0.089 | 0.085 | 0.088 | 0.082 | 0.081 | 0.031 | 0.088 | 0.091 |
| Ce | 0.204 | 0.208 | 0.208 | 0.204 | 0.208 | 0.195 | 0.186 | 0.174 | 0.156 | 0.168 | 0.150 | 0.152 | 0.040 | 0.183 | 0.177 |
| Pr | 0.017 | 0.019 | 0.017 | 0.018 | 0.016 | 0.017 | 0.017 | 0.017 | 0.015 | 0.015 | 0.007 | 0.011 | 0.002 | 0.016 | 0.015 |
| Nd | 0.044 | 0.047 | 0.044 | 0.045 | 0.042 | 0.041 | 0.046 | 0.046 | 0.034 | 0.041 | 0.039 | 0.027 | 0.004 | 0.045 | 0.043 |
| Sm | 0.002 | 0.002 | 0.001 | 0.002 | 0.001 | 0.003 | 0.002 | 0.002 | 0.001 | 0.001 | 0.004 | 0.000 | 0.000 | 0.002 | 0.003 |
| Th | 0.003 | 0.003 | 0.003 | 0.005 | 0.003 | 0.004 | 0.006 | 0.006 | 0.005 | 0.005 | 0.004 | 0.009 | 0.003 | 0.006 | 0.006 |
| U | 0.001 | 0.002 | 0.000 | 0.000 | 0.000 | 0.000 | 0.001 | 0.001 | 0.001 | 0.000 | 0.001 | 0.001 | 0.002 | 0.000 | 0.001 |
| SUM A-site | 1.011 | 1.039 | 1.006 | 1.010 | 1.020 | 1.015 | 1.043 | 1.036 | 1.007 | 1.031 | 1.017 | 1.022 | 1.026 | 1.036 | 1.012 |
| Ti | 0.893 | 0.890 | 0.884 | 0.885 | 0.889 | 0.885 | 0.858 | 0.840 | 0.772 | 0.810 | 0.813 | 0.708 | 0.243 | 0.867 | 0.859 |
| Nb | 0.090 | 0.086 | 0.098 | 0.100 | 0.094 | 0.101 | 0.114 | 0.138 | 0.214 | 0.174 | 0.172 | 0.281 | 0.742 | 0.114 | 0.125 |
| Ta | 0.005 | 0.004 | 0.008 | 0.006 | 0.005 | 0.005 | 0.006 | 0.006 | 0.009 | 0.008 | 0.004 | 0.009 | 0.007 | 0.005 | 0.005 |
| Fe | 0.013 | 0.007 | 0.013 | 0.009 | 0.011 | 0.007 | 0.008 | 0.003 | 0.001 | 0.000 | 0.017 | 0.001 | 0.006 | 0.003 | 0.007 |
| SUM B-site | 1.001 | 0.988 | 1.002 | 0.999 | 0.998 | 0.997 | 0.987 | 0.986 | 0.996 | 0.992 | 1.005 | 0.999 | 0.997 | 0.989 | 0.996 |
| Total Cations | 2.012 | 2.027 | 2.008 | 2.009 | 2.018 | 2.012 | 2.029 | 2.022 | 2.003 | 2.023 | 2.022 | 2.021 | 2.024 | 2.025 | 2.007 |
| % lueshite | 9.6 | 9.2 | 10.7 | 10.7 | 10.0 | 10.7 | 12.3 | 14.6 | 22.4 | 18.3 | 17.8 | 29.0 | 75.5 | 12.1 | 13.1 |
| % loparite | 73.6 | 76.1 | 75.1 | 74.3 | 74.7 | 71.3 | 69.5 | 66.6 | 58.6 | 63.2 | 57.3 | 54.1 | 15.6 | 67.7 | 66.6 |
| % tausenite | 2.0 | 2.5 | 2.5 | 2.4 | 2.7 | 4.3 | 6.4 | 7.9 | 9.3 | 8.2 | 4.2 | 3.4 | 5.2 | 6.6 | 6.8 |
| % perovskite | 14.7 | 12.2 | 11.7 | 12.5 | 12.6 | 13.6 | 11.9 | 10.9 | 9.7 | 10.3 | 20.7 | 13.4 | 3.8 | 13.6 | 13.5 |

Analysis 1 is average of 4 spot analyses. *Cum* cumulus phase. *Inter* intercumulus phase. Mg, Al, P, K, Cr, Zr, Gd, Hf, Pb were all below microprobe detection limits

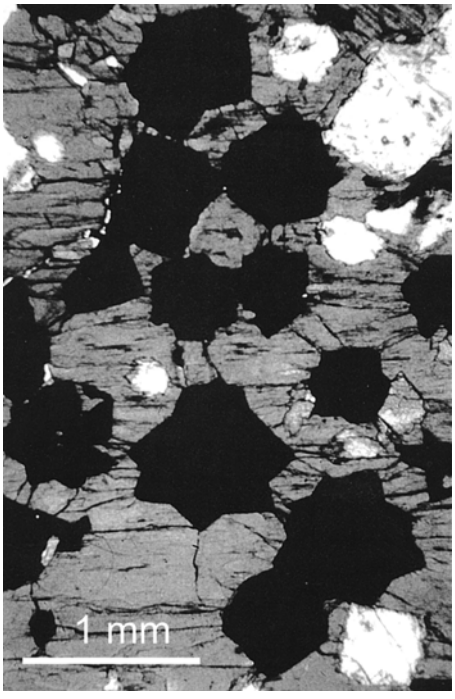


Fig. 3. Photomicrograph of loparite ore. Black: loparite; grey: pyroxene; white: nepheline. Plane polarised light. The loparite crystals are 0.7–0.8 mm across

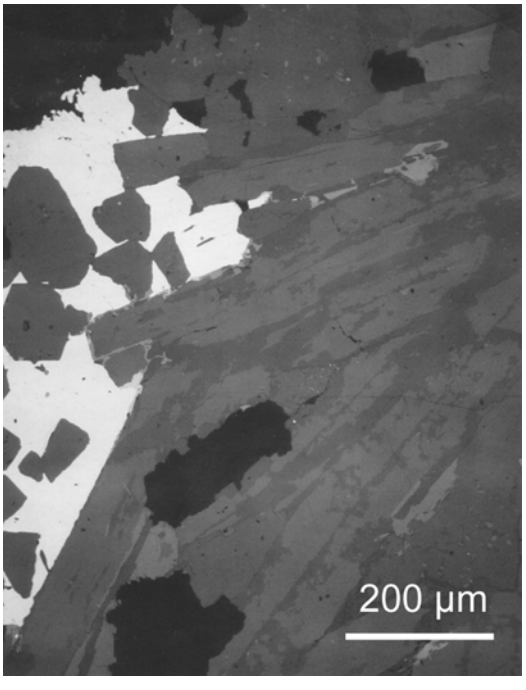


Fig. 4. Backscattered electron image showing loparite (white) interstitial to pyroxene (grey), nepheline and feldspar (dark grey) from the lowest part of the Differentiated Complex. The black areas are holes in the section

In the Eudialyte Complex loparite forms euhedral cumulus crystals only in the lower zone (about 150 m thick). In the upper parts of this complex loparite is commonly developed in the interstices of other minerals as irregular and poikilitic crystals. Idiomorphic cumulus loparite in the upper part of the Eudialyte Complex is

very rare. This feature of loparite morphology in Phase III was also reported by *Ifantopulo* and *Osokin* (1979).

Commonly, loparite is partially replaced by late-magmatic fibrous aggregates of lomonosovite-murmanite, lamprophyllite, mosandrite, nenadkevichite, steenstrupine and phosphates of REE, Ca and Sr.

## Compositional evolution of loparite related to magmatic fractionation trends

Loparite was first documented in the Lovozero Massif by *Ramsay* and *Hackman* (1894) and subsequently studied in detail by a number of researchers (*Vorob'eva*, 1938; *Gerasimovsky* and *Kostyleva*, 1937; *Vlasov* et al., 1966; *Smirnov*, 1976; *Kravchenko* et al., 1974; *Ifantopulo* and *Osokin*, 1979; *Kogarko* et al., 1996; *Mitchell* and *Chakhmouradian*, 1996). Some systematic changes were noted in the loparite composition through the Lovozero differentiated complex, but the majority of the earlier studies were based on analyses of loparite concentrates separated from polymineral fractions.

Progress in the accurate measurement of major and trace elements in individual mineral grains by electron microprobe now makes it possible to study the zoning and chemical variation of the loparite in individual grains within particular horizons and through the vertical section of the differentiated and eudialyte-bearing complexes. The analyses were made on a Cameca SX50 wavelength-dispersive electron microprobe at the Natural History Museum, London. Operating conditions were an accelerating voltage of 15 kV and 20 nA probe current. Standards used were a combination of natural minerals, synthetic compounds and pure metals, which included synthetic $NaNbO_3$, $SrTiO_3$, $CaTiO_3$, and individual REE-doped glasses for the major components. Background positions were carefully selected to avoid interferences, particularly for the REE, and inter-element empirical corrections made following the procedure in *Williams* (1996). Count times for peak and backgrounds varied with the element being analysed: 10 s for major elements, and 30 to 50 s for minor elements including middle to heavy REE, Ta, and Actinide elements. Under the conditions employed, errors were typically $\pm 5\%$ for major elements, and $\pm 10\%$ for minor elements, depending on the extent of any interference corrections that were made.

Loparite is a member of the perovskite structural group which may be written as $ABO_3$ (or $A_2B_2O_6$), in which A includes Ca, Sr, Na, REE and Ba and B includes Ti, Nb, U, Th and Ta. In spite of the rather variable composition, the majority of natural loparites have compositions which fall within the quaternary system represented by four major end-member components: perovskite ($CaTiO_3$), tausonite ($SrTiO_3$), lueshite ($NaNbO_3$) and loparite ($Na_{0.5}Ce_{0.5}TiO_3$), see *Mitchell* (1996) for a recent classification scheme.

The variation in the composition of the loparite from Lovozero can be seen in the lueshite-perovskite-loparite ternary diagram (Fig. 5). This diagram illustrates the differences in composition in loparite between the two complexes, and results from its evolution from a cumulus to intercumulus phase (indicated by the arrow #1), together with, for one grain, an extreme fractionation trend within trapped interstitial magma. In Fig. 5, the majority of analyses plot in the field of loparite, as

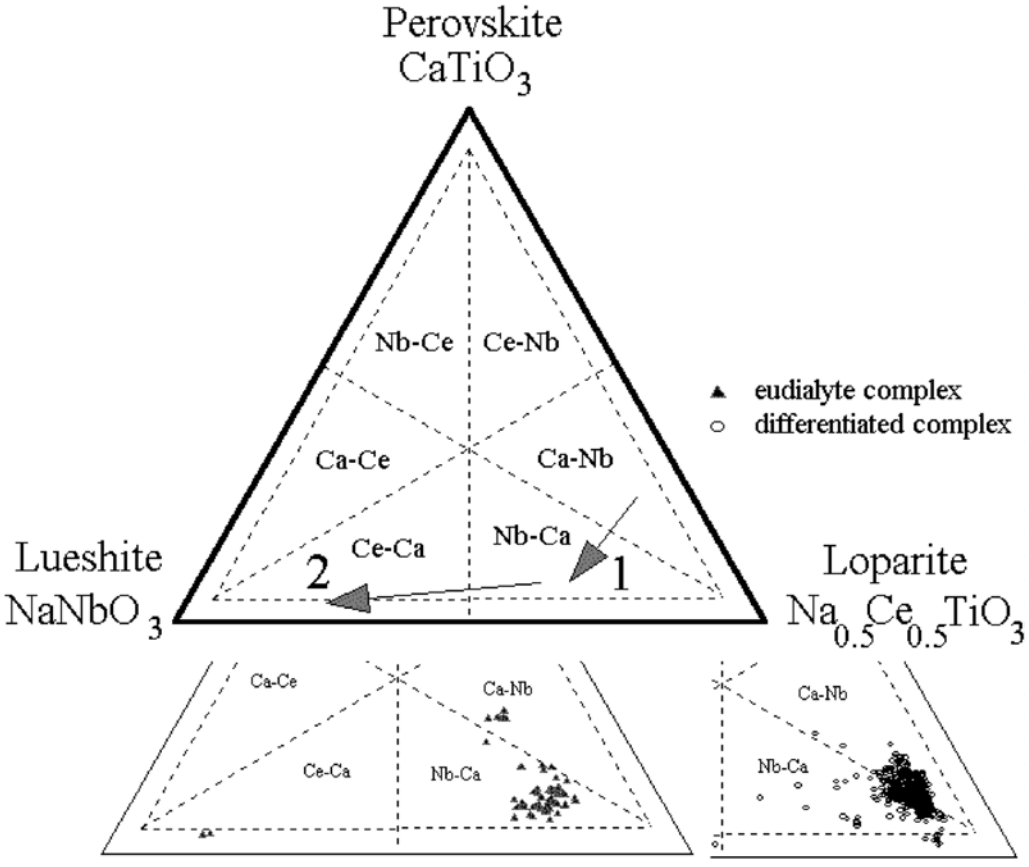


Fig. 5. Plot of loparite composition in terms of the lueshite, perovskite and loparite end-member molecules. Open circle symbol denotes loparite from Differentaited Complex and filled triangle loparite from Eudialyte Complex. The change of composition of the loparite with increasing height through the Lovozero intrusion is indicated by the arrow #1, and the compositional change within trapped, interstitial magma by arrow #2

was shown by earlier workers (*Gerasimovsky* and *Kostyleva*, 1937; *Vlasov* et al., 1966; *Kogarko* et al., 1996; *Mitchell* and *Chakhmouradian*, 1996). However, some compositions lie in the fields of niobian loparite and cerian lueshite (nomenclature from *Mitchell*, 1996).

The composition of loparite reflects the fractional crystallisation of the highly alkaline melt. In this work, the evolution of the Lovozero magma was monitored through about 2,350 m of layered nepheline syenites using the loparite compositional changes, which have been plotted as a function of the structural depth in the intrusion (Fig. 6).

As has been shown by many authors (e.g. *Henderson*, 1975; *Hunter*, 1996) the compositions of cumulus phases in layered intrusions might be changed dramatically by subsequent reaction with intercumulus melts and by re-equilibration processes. This factor has the effect of producing significant changes within those elements most affected by reactions with intercumulus melt, and contributes significantly to the vertical ''scatter'' seen in Fig. 6. In order to minimize the influence of

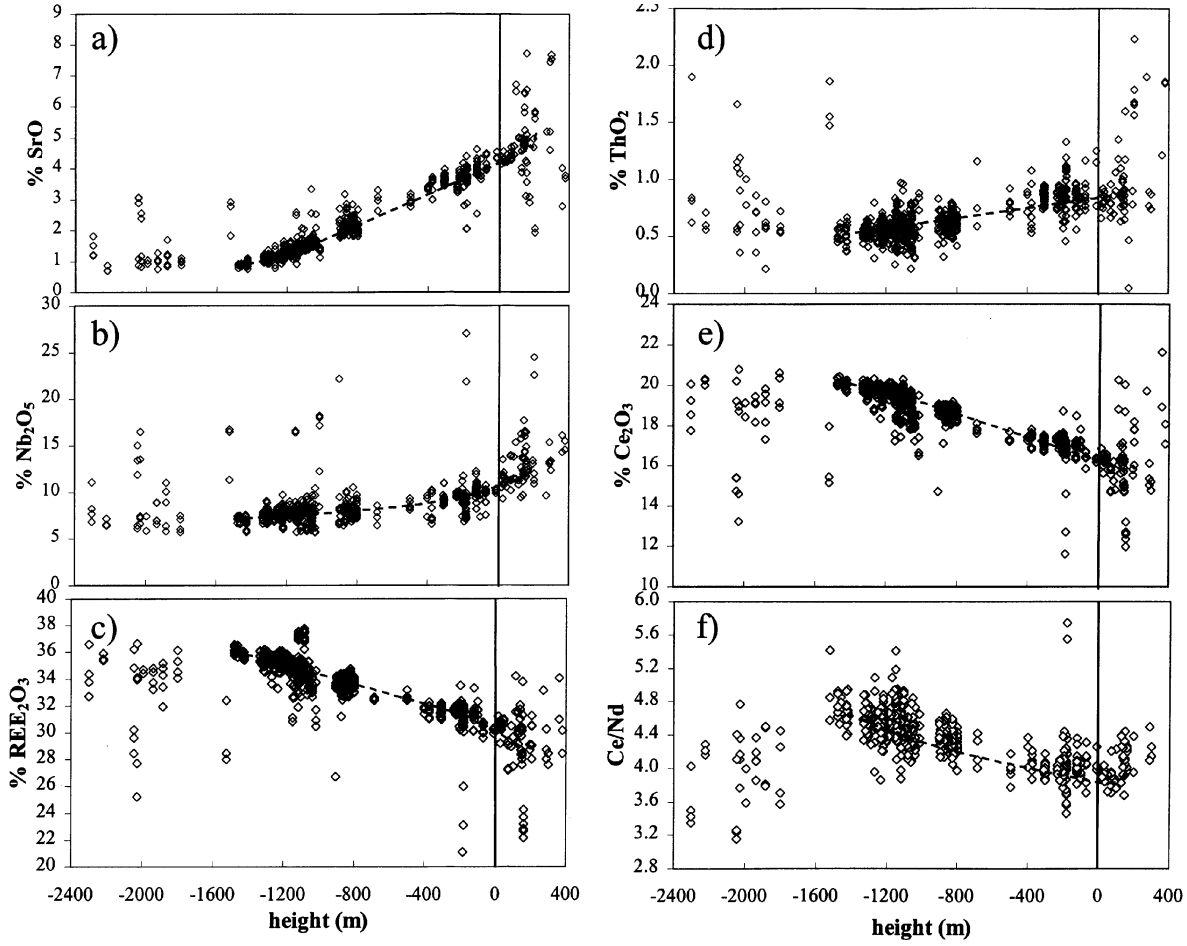


Fig. 6. Chemical variation of loparite plotted against height in the Lovozero complex. The line at 0 metres is taken at the top of the Differentiated Complex. **a** SrO, **b** $Nb_2O_5$, **c** total $REE_2O_3$, **d** $ThO_2$, **e** $Ce_2O_3$, **f** Ce/Nd

post-cumulus factors on genuine cryptic variations in loparite composition, we analysed about 400 grains of loparite from 63 samples from the so-called 'ore layers', where loparite occurs mostly as a cumulus mineral at modal proportions $>$ 1–2 vol.%, and where their stratigraphical positions are well-constrained. We also investigated loparite in about 50 further thin sections, mainly from drill-cores, from the Differentiated and Eudialyte Complexes.

Moving stratigraphically upwards through the intrusion the cumulus loparite becomes progressively enriched in Sr, Nb, Ta, Th and Na and depleted in Ca, Fe, Ti, total REE. This is the principal trend of cumulus loparite evolution in Lovozero, which is observed through some 1600 m of the intrusion. The degree of scattering of the compositional data is because some of the loparite analysed in this zone is intercumulus, seen from thin section examination (and backscattered electron images), where it has crystallised within localised, trapped, interstitial melt.

Table 3. *Chemical variation across a zoned, interstitial loparite grain*

| | Centre of grain | | Rim of grain | |
|---|---|---|---|---|
| SrO | 0.83 | 2.78 | 2.57 | 2.40 |
| $ThO_2$ | 0.36 | 0.83 | 0.60 | 1.19 |
| $Nb_2O_5$ | 6.60 | 12.76 | 13.56 | 16.50 |
| $Ce_2O_3$ | 20.70 | 13.32 | 14.61 | 13.23 |
| $Nd_2O_3$ | 4.36 | 3.46 | 3.88 | 3.17 |
| Nb:Ta ratio | 13.8 | 22.6 | 26.1 | 48.5 |
| Ce:Nd ratio | 4.7 | 3.8 | 3.8 | 4.2 |

In Figs. 6a–f, where oxides, or element ratios are plotted against depth, the zero line is taken at the top (contact) of the Differentiated Complex with the Eudialyte Complex. All depths in the differentiated complex are expressed as negative numbers, and in the Eudialyte Complex as positive numbers (see also Fig. 2). Our petrographic data indicate that loparite is a cumulus phase in the Differentiated Complex from a depth of about −1500 m up to about +150 in the Eudialyte Complex. As mentioned above, loparite is intercumulus in the lower part of the Differentiated Complex (from −2300 to −1500 m), and its composition here reflects crystallisation within an evolving trapped liquid, which resulted in large variations in its composition (Fig. 6 shows the major variables). It is noteworthy that the same trends for Sr, Nb, Th, and REE that are observed for cumulus loparite in the layered sections of the massif, can be demonstrated within one interstitial loparite grain. In the lowest part of the Differentiated Complex (2029 m depth) in one zoned grain of interstitial loparite the values shown in Table 3 were obtained (across the grain from the centre to the edge). Comparison of these data with the distribution of Nb, Sr, Th and REE in cumulus loparite throughout the layered section of the Lovozero intrusion indicates that the complete evolution of this large magma chamber can be represented in one interstitial loparite grain.

During the evolution of the Eudialyte complex, when about 30% of the magma had crystallised, lamprophyllite is likely to have become a cumulus phase, together with nepheline, K-feldspar, aegirine, eudialyte and arfvedsonite. Petrographic investigations show that lamprophyllite in the lower part of the Eudialyte Complex (to approximately 100–150 m from the contact with Phase II) occurs as irregular plates or interstitial crystals, but in the upper part the abundance of lamprophyllite increases substantially and it forms euhedral, elongate crystals among aegirine needles. Lamprophyllite is a major sink for Ti and Sr, containing up to 30 wt% $TiO_2$ and 16 wt% SrO, thus early crystallisation of lamprophyllite will result in a depletion of these elements in the fractionated magma. The crystallisation of lamprophyllite led to a decrease in the content of Sr in the cumulus loparite in the upper part of Phase III (for instance, to 1.9% SrO) at depths of 205 m (from the contact with the Differentiated Complex).

Our investigation also indicates that in the uppermost part of the Eudialyte Complex pyrochlore, containing up to 52 wt% $Nb_2O_5$, forms euhedral crystals and so probably also became a cumulus phase. As a result of the appearance of cumulus lamprophyllite and pyrochlore the field of crystallisation of loparite dramatically

decreased. This feature also may be related to an increase in the alkalinity of the magmatic system at this stage of the evolution of the intrusion. Experimental data of *Kogarko* et al. (1982) have shown that the concentration of loparite at the eutectic in the nepheline-loparite system is ~17 wt%, but in the system lueshite-nepheline the content of the more alkali-rich lueshite reaches 48%. Saturation of the alkaline melt in more lueshite-rich loparite takes place at a much lower temperature which led to the interstitial crystallisation of loparite. This is probably the reason for the wide scatter of the Sr, Nb, REE and Th data of the loparite from the upper part of the Lovozero intrusion (Figs. 6a–e).

The Nb:Ta ratio (not shown in Fig. 6) in the cumulus loparite increases continuously upwards from an average value close to 12 in the lower part of the Differentiated Complex to 32 in some loparite grains from the Eudialyte Complex. This overall trend has been confirmed from preliminary laser-ablation ICPMS data on a smaller sub-set of the loparite samples. Very high Nb:Ta ratios up to 48.5 were observed in one grain of interstitial loparite of Phase II and exceptionally high, up to 299, in intercumulus loparite of Phase III. It is interesting to note that pyrochlore from this sample has also a very high Nb:Ta ratio of 326. In loparite from pegmatite at Khibina the Nb:Ta ratio is also high (38.5).

Cumulus loparite is the major host of REE in the Lovozero peralkaline magma, particularly in the Differentiated Complex. The mineral-mineral partition coefficient of REE in loparite and apatite which are in equilibrium, they are both cumulus minerals in Phase II, is relatively high i.e. for Ce = 5.5, for Nd = 4.3 and for Sm = 1.

The initial Ce:Nd ratio in the primary magma of the Differentiated Complex, according to the data of *Balashov* and *Turanskaya* (1960), is 3.4. With increasing stratigraphic height the Ce:Nd ratio in cumulus loparite decreases slightly from a mean value of 4.7 in the lower part of the differentiated complex to a mean of 4.0 in loparite from the upper part (Fig. 6f). In Phase III however, this trend is reversed with an inverse correlation in the Ce:Nd ratio with height. Consequently, crystallisation of loparite will decrease the Ce:Nd ratio in the melt during its crystallisation.

This study shows that many interstitial minerals, such as monazite, vitusite, steenstrupine and mosandrite, also have higher Ce:Nd ratios than the primary melt of the Differentiated Complex (i.e. $> 3.36$), thus their crystallisation will also decrease the Ce:Nd ratio in the residual liquid. The migration of less dense interstitial melt through the pores of the partly consolidated rocks, as a result of compaction and convection within the settled crystals, is an important process in layered intrusions (*Naslund* and *McBirney*, 1996), and such melts may interact with the main portion of the magma. Thus, in the case of an open system, in respect of movement of residual melt, the crystallization of interstitial, REE-bearing mineral phases from this interstitial melt would also have contributed to a decrease in the Ce:Nd ratio of the Phase II melt during differentiation.

It should be noted that the average Ce:Nd ratio in the rocks of a very large pegmatite body of Phase II falls as low as 1.54 (*Gerasimovsky* et al., 1966). An inversion in the trend of the Ce:Nd ratio in loparite during the evolution of the Eudialyte Complex (Fig. 6f) may be attributed to the early crystallisation of eudialyte which here becomes a major cumulus phase. The Ce:Nd ratio of the eudialyte is approximately 2.0 throughout the Eudialyte Complex, and its crystal-

lisation will increase the initial Ce:Nd ratio in the melt and consequently affect its ratio in loparite crystallising from this melt.

The composition of loparite from the poikilitic sodalite syenite body in the lower part of the Differentiated Complex (Phase II) was also investigated (analysis 1, Table 2). Loparite from this sample contains very low Na and Nb, and high total REE. The poikilitic sodalite syenite sample is from an isolated oval-shaped body approximately 16 m in diameter; it displays sharp contacts against the surrounding juvite and does not have feeding channels. It consists of sodalite (∼60%), microcline and albite (∼15%), aegirine and arfvedsonite (∼5%), nepheline (∼15%) and accessory eudialyte, villiaumite, loparite, lorenzenite, monazite and thorianite. As has been demonstrated (*Kogarko* et al., 1974) the composition of sodalite syenites lies in the immiscibility field in the system nepheline-albite-halite, and many geological and geochemical features of these rocks are consistent with the model of poikilitic sodalite syenite originating by a process of liquid immiscibility. The evidence includes very high concentrations of chlorine and fluorine, the presence of primary micro-inclusions containing halite, and characteristic distribution patterns of some rare elements between the country rocks and poikilitic sodalite syenites (*Gerasimovsky* et al., 1966).

The separation of immiscible liquids demands equilibrium not only between them, but also between all the solid phases. Our data show that the composition of loparite is similar in both the poikilitic sodalite syenites and the enclosing juvite (analysis 2, Table 2). Thus, these data are in general agreement with other geochemical and petrological evidence of the major role of liquid immiscibility in the origin of sodalite syenites.

## Zoning in loparite

Loparite zoning was considered earlier from some Lovozero samples by *Mitchell* and *Chakhmouradian* (1996), but was restricted mainly to descriptions of core-rim zonation. Our study from an extended range of loparite samples has shown that individual crystals can display very complex zoning, best illustrated using backscattered electron images (Figs. 7a and b). Darker (lower mean atomic number) zones are usually enriched in Na, Nb and Sr, while the lighter zones are characterised by higher concentrations of REE, Th, Ti and Ca. Several types of zoning are distinguishable.

1. Marginal zoning, in which there is enrichment in Sr, Nb and Na in the outer rim (Fig. 7a).
2. Reverse zoning, in which the outer rim is depleted in Sr, Nb and Na.
3. Oscillatory zoning in which there is repetition of zones enriched and depleted in Sr, Nb and Na.
4. Sector zoning.
5. Irregular zoning (Fig. 7b).

The marginal zoning is undoubtedly caused by loparite crystallisation in equilibrium with a restricted amount of interstitial melt, when the loparite rapidly becomes enriched in the lower temperature components lueshite and tausonite. The same trend was reported by *Veksler* et al. (1989) in experimental studies involving

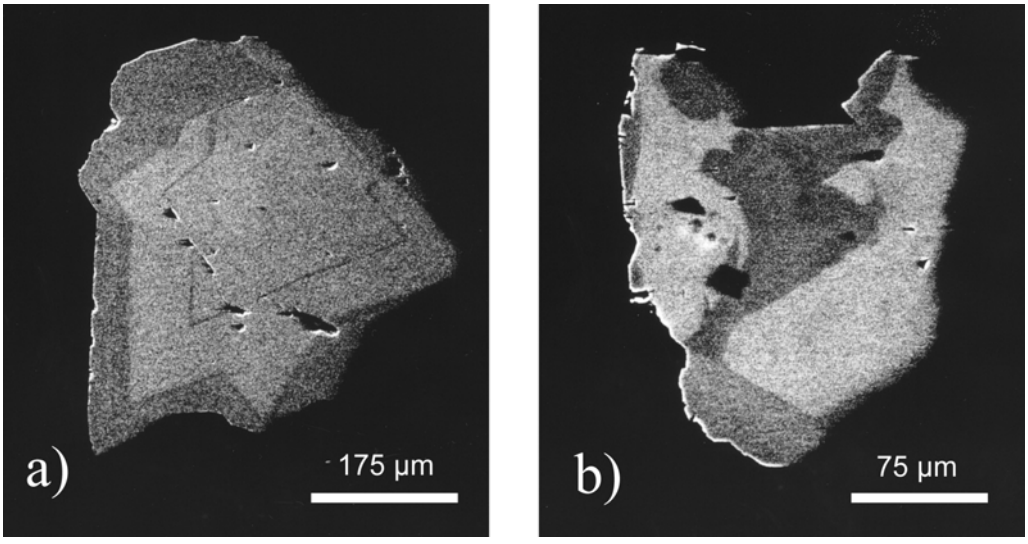


Fig. 7. Backscattered electron images of loparite showing **a** marginal zoning, and **b** patchy zoning

decreasing temperatures. Reverse zonation is probably the result of crystallisation of the loparite in interstitial melt simultaneously with mineral phases having higher partition coefficients for Sr, Nb and Na. These minerals include lamprophyllite, Sr-apatite, murmanite-lomonosovite, pyrochlore and nenadkevichite, which are abundant as interstitial minerals in rocks of Phases II and III.

Oscillatory zonation is the result of the interplay of several factors such as the variations in rates of crystal growth of loparite and minerals competing for the major components of loparite, differential element diffusion rates, and localised disequilibrium conditions adjacent to growing loparite crystal faces. Such mechanisms have been described previously in peralkaline magmas (*Kogarko* and *Volkov*, 1963), and are a relatively common feature described in a range of minerals from other magmatic environments.

One of the reasons for the irregular and sector zoning might be the partial recrystallisation of the loparite after accumulation. Such processes are widespread in cumulus rocks of layered intrusions (*Hunter*, 1996). Another factor that may contribute to these types of zoning is the formation of glomeroporphyritic crystal aggregates in the melt, which retain their distinctive composition in the sedimented mush where they anneal and recrystallise into zoned crystals. These aspects will be considered further in a separate publication.

## Loparite – melt reactions

During crystallisation of agpaitic nepheline syenite melts, the alkalinity increases continuously. High alkalinity prevents the separation of volatile components, i.e. $H_2O$, F, Cl, S etc., and rare elements into the gas phase (*Kogarko*, 1977), which is a fundamental geochemical feature of agpaitic magmas. The very high solubility of water in agpaitic melts (*Kogarko* et al., 1977 and *Kogarko*, 1990) will cause the very

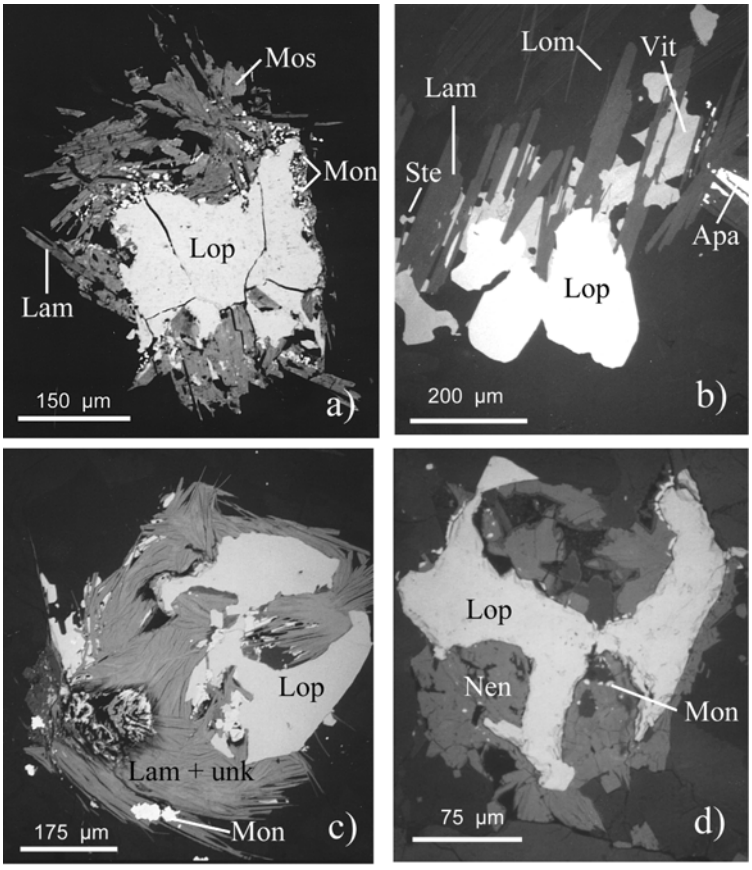


Fig. 8. Backscattered images showing reactions of loparite with residual melt. **a** Loparite (Lop) replaced by acicular lamprophyllite (Lam), platy mosandrite (Mos) and 5–10 μm monazite crystals (Mon). **b** Loparite (Lop) replaced by acicular lamprophyllite (Lam), lomonosovite (Lom), irregular crystals of vitusite (Vit), steenstrupine (Ste) and REE, Sr-rich apatite (Apa). **c** Loparite is replaced by Ba lamprophyllite (Lam) intergrown with an unknown phase (unk), and monazite (Mon). **d** Loparite (Lop) replaced by nenadkevichite (Nen) which includes small pyroxenes (black), and 5–10 μm monazite crystals (Mon)

gradual transition from magmatic peralkaline residual melt into hydrothermal solution (brine). Extremely high concentrations of F and Cl (*Gerasimovsky* et al., 1966) enhance this process. The accumulation of volatile components in the melt, but not in the vapour phase, is the reason for the extremely low temperature of the solidus of these rocks, approximately 425 °C (*Kogarko* et al., 1974), and a very prolonged interval of agpaitic rock crystallisation. This feature facilitates the post-cumulus reactions.

Our study has demonstrated that loparite primocrysts may not only change their composition, but may be replaced by other minerals during the late stages of high alkaline magma evolution (Figs. 8a–d).

The petrography indicates that the urtites are typical adcumulates, usually with a very small percentage of intercumulus material, and that compaction was an

important process in their formation. The foyaite and lujavrite, in contrast, contain much more interstitial material and loparite here is more commonly replaced by another phase.

We have recognised seven reactions between loparite and the trapped residual liquid ($L_1$ and $L_2$). Mineral formulae are given in Table 1.

1. Loparite + $L_1$ = Mosandrite + Lamprophyllite + Monazite + $L_2$
2. Loparite + $L_1$ = Barytolamprophyllite + Lomonosovite + Vitusite + Steenstrupine + REE, Sr-rich apatite+$L_2$
3. Loparite + $L_1$ = Monazite + Cerite + Barytolamprophyllite + $(Na,K)_2(Ca,Mg,Fe,Mn)_{0.88}Ba_{0.93}Nb_{0.77}Ti_2Si_{4.09}O_{17}(F,OH,H_2O)_x$+$L_2$ unknown phase
4. Loparite + $L_1$ = Nenadkevichite + Monazite + $L_2$
5. Loparite + $L_1$ = Nordite+Lomonosovite + $L_2$
6. Loparite + $L_1$ = Vuonnemite + Monazite + $L_2$
7. Loparite + $L_1$ = Barytolamprophyllite + Ba, Si-rich belovite + $L_2$

These reactions indicate a dramatic increase in the concentrations of volatiles (F, $H_2O$), Na, P, Th, Ba and Zn in the residual interstitial melt in which loparite became unstable. The migration of the interstitial melt from the urtite layers is probably one of the reasons for the preservation of the loparite ore in these rocks. These aspects will be considered further in a separate publication in which full chemical analyses will be presented.

## Mechanisms of loparite fractionation

The large amount of data on layered intrusions from different parts of the world accumulated during recent decades has provided new evidence and mechanisms to explain the observed phenomena (*Parsons*, 1987). The role of *in situ* processes has been considered including different patterns of convection, flow segregation, nucleation density, compaction, textural equilibration and recrystallisation. However, the origin and differentiation of layered intrusions still remains largely unresolved because of the complexity of this process and participation of many different genetic mechanisms. The compositions of cumulus minerals in layered intrusions provide invaluable information about the fractionation processes and melt evolution in the magma chamber.

Given the concentrations of a component in loparite as a function of depth in the layered intrusion and assuming that the behaviour of this component obeys the Rayleigh law (ideal fractional crystallisation with constant partition coefficients), we may estimate partition coefficients and the fraction of loparite in the total mass of crystallising solid phases. The Rayleigh equation is:

$$C_L = C_O * (F_L)K_B - 1$$

where $C_L$ is the concentration in melt at a given stage; $C_O$ is the initial concentration in the melt prior to crystallisation (taken here as an average abundance in the intrusion); $F_L$ is the fraction of melt remaining in the system at a given moment, calculated as the ratio of distance of a given layer from the top of the intrusion

divided by the thickness of the intrusion, and $K_B$ is the bulk (weighted average) partition coefficient.

Where $K_{lop}$ is the partition coefficient of some element in loparite $= C_{lop}/C_L$ the concentration in loparite $(C_{lop})$ may be expressed as:
$C_{lop} = K_{lop} * C_O * (F_L)K_B - 1$, or in the logarithmic form:-

$$\ln(C_{lop}) = \ln(K_{lop} * C_O) + (K_B - 1) * \ln(F_L).$$

From the available analytical data we estimate $(K_B - 1)$ and $\ln(K_{lop} * C_O)$ applying the least squares procedure to the linear regression of $\ln(C_{lop})$ against $\ln(F_L)$. For REE and a number of other components we make the assumption that loparite is the only crystallising phase which incorporates these elements in substantial amounts, and therefore

$$K_B = r_{lop} * K_{lop}$$

where $r_{lop}$ is the fraction of loparite in the total mass of crystallising solid phases.

Using the data on the distribution of Sr, REE, Nb, Ta and Th in loparite we obtained estimated values for the fraction of loparite in the total mass of crystallizing solid phases in the Differentiated complex to be in the range of 0.6–4% which is consistent with the experimental data of *Kogarko* et al. (1983) who estimated the proportion of loparite in eutectic with lujavrite to be 1–2%.

The calculated partition coefficients between loparite and alkaline melt for Sr, REE, Nb, Ta and Th are 22.6, 100–157, 80, 85, 133 respectively. The bulk partition coefficients were estimated to be for Sr = 0.52–0.38, REE = 1.06–0.91, Nb = 0.87, Ta = 0.92, Ti = 1.01, and Th = 0.77. The partition coefficients of Ce and La for loparite/alkaline melt have also been obtained, based on the distribution of these elements between cumulus loparite and apatite from the same Lovozero samples. *Wörner* et al. (1983) have reported melt distribution coefficients for rare earths for apatite/Laacher See phonolite i.e. La, 14.4 and Ce, 24.3, which we used for calculation, because of the similarity in composition of this rock with Lovozero. The estimated loparite/melt partition coefficients of La and Ce (80–135) for Lovozero are close to the previously calculated data, given above (i.e. 100–157).

In spite of the relatively low concentrations of the loparite component necessary to saturate peralkaline magma (1–2%) according to the experimental data (*Kogarko* et al., 1983; *Veksler* et al., 1989), the initial Lovozero melt was not saturated with respect to loparite, which is confirmed by the fact that loparite is absent from Phase I (*Gerasimovsky* et al., 1966). In Phase II, loparite became a cumulus phase only after about 35% crystallisation of the magma. At depths below about −1500 m in Phase II, loparite is an interstitial phase and its composition reflects the rapid evolution of trapped melt. In this part of the intrusion the main Ti and Nb cumulus phases are titanite, ilmenite and titanomagnetite. With the increasing alkalinity and concentration of REE and Nb in the melt, loparite started to crystallise as a cumulus phase and its composition changed systematically through about 1500 m towards the top of the intrusion (Fig. 6). This systematic change correlates with stratigraphic level and with an increase in the lower temperature components lueshite and tausonite (Na, Sr, Nb). There are no discontinuous changes in the cumulus loparite composition throughout the Differentiated Complex, which indicates the absence of

magma replenishment in this intrusion, but instead implies a closed system fractionation. The initial melt of the Eudialyte Complex, in contrast to the Differentiated Complex, is saturated with respect to eudialyte, which is a cumulus phase throughout. As outlined above, lamprophyllite probably became a cumulus phase after crystallisation of approximately 30% of the Eudialyte complex. Loparite still occurs, but only as a relatively rare phase. However, the experimental phase relationships between loparite and lamprophyllite are not known for this stage. The reaction of loparite with peralkaline interstitial melt producing lamprophyllite in the Differentiated Complex suggests that in the more peralkaline Eudialyte complex, this reaction controls the whole of the evolution of the later stages of the melt, which precludes the formation of loparite accumulation (i.e. loparite ore) in the rocks of phase III.

From the observed data of the significant cryptic variation in loparite through the intrusion (Fig. 6), it is clear that differentiation from lower to higher levels was the dominant process occurring in the magma chamber, and therefore that the loparite-rich horizons were formed during the magmatic stage. Geological evidence, including continuous layers of lujavrite, foyaite and urtite, together with isotopic studies (*Kogarko* et al., 1983; *Kramm* and *Kogarko*, 1994), point to fractionation of the Lovozero magma within a closed magma chamber. Plots of Sr, Nb, REE and Th concentrations against depth (Figs. 6a–d) also indicate the closed character of the fractionation at Lovozero. The linear correlation of log-element concentrations in plots of cumulus loparite against log-depth (not shown) testify to the relatively constant bulk partition coefficients of these elements in loparite in the Differentiated Complex, which are independent of changes in melt composition. These data show a good correspondence with the experimental data of *Kogarko* et al. (1983) and *Veksler* et al. (1984), which indicates that the partition coefficients of Sr, Nb and REE in the equilibrium loparite-lujavrite-melt and loparite-nepheline-melt did not change. As outlined above, bulk partition coefficients for LREE, HREE and Sr in loparite changed in Phase III, because here eudialyte, lamprophyllite and pyrochlore became cumulus mineral phases. Thus, it is possible to suggest that fractional crystallisation, combined with continuous settling of loparite, was the most important process responsible for the observed chemical trend of loparite through the stratigraphic section and for the genesis of the loparite ore. The sorting phenomenon of loparite grains in the ore layers supports this conclusion.

As demonstrated by *Sparks* et al. (1993) in magmatic systems containing minerals with different settling velocities, and different critical concentrations, a sequence of layers can result from steady convection and steady cooling. Crystals in melts may remain in suspension only until the settling velocity is small as compared with the velocity of convective currents (*Marsh* and *Maxey*, 1985; *Kogarko* and *Khapaev*, 1987; *Sparks* et al., 1993). We may speculate that the formation of rhythmic units in Phase II, consisting of loparite-bearing urtite, foyaite and lujavrite, may be attributed to sedimentation from relatively steady convection. During this process the alkaline magma contained cumulus phases, including nepheline, loparite, feldspar, aegirine and amphibole.

Petrographic examination of urtite layers clearly demonstrates the striking cumulate textures of these layers where cumulus nepheline and loparite are

concentrated. Loparite, as the most dense cumulus phase, sank to the lowest part of the urtite layers and even, in some cases, penetrated into the upper zone of the partially solidified underlying lujavrite. Smaller grain-sized nepheline and feldspar crystals, accumulated later forming the foyaite layers having an orthocumulate texture, using the nomenclature proposed by *Hunter* (1996). Subsequently, aegirine, which usually forms smaller needle-like crystals, started to crystallise and sink simultaneously, or even later, with these minerals so that foyaite gradually graded into lujavrite. The overlying urtitic units probably formed from successive convection, or sedimentation (*Sparks* et al., 1993), pulses resulting in sharp contacts with the underlying lujavrite, examples of which can be seen clearly throughout the Differentiated Complex. There is evidence for sorting of the minerals within some of the units such that larger crystals accumulate in the lower part of the urtite layers, whereas smaller crystals are confined to the upper part of the lujavrites. The succession of rocks in these units was probably partially facilitated by the very large field of crystallisation of nepheline and feldspar in the Lovozero peralkaline magmatic system (*Kogarko*, 1977).

This hypothesis for the formation of rhythmic layering is supported firstly by the correlation of the thickness between urtite, foyaite and lujavrite in each unit, the disturbance of this regularity probably being related to magmatic erosion, and secondly, by the presence of centimetre-scale lamination, this being especially well exhibited by feldspar and aegirine. These field observations we interpret as being evidence for the existence of convection currents within the magma chamber. Deviation from this regularity might be attributed to the fluctuations in the degree of compaction, strength of convection, and different other factors, during the formation of loparite-bearing layers.

As mentioned above, the high alkalinity of the Lovozero magma and the accumulation of volatile components in the peralkaline melt, but not in the fluid phase, was the main reason for the gradual transition from the magmatic to the hydrothermal stage and the very long period of crystallisation. This geochemical feature of the peralkaline magma system initiated the wide-scale development of the late-stage processes such as recrystallisation, reactions with interstitial melt and textural equilibration, which partly overprinted the characteristic primary features of the loparite in the Lovozero intrusion.

## Conclusions

From the data it is clear that there is a significant systematic cryptic variation in cumulus loparite throughout the Lovozero layered intrusion, so that fractional crystallisation combined with settling of the fractionating phases, in a closed system, was the dominant differentiation process of the Lovozero magma. Thus, the massive loparite deposits are magmatic in origin, and not the result of a metasomatic event as suggested by some earlier workers (e.g. *Eliseev* and *Fedorov*, 1953).

The process of fractional crystallization is recorded in the composition of the loparite throughout the whole layered intrusion. The composition of intercumulus loparite reflects crystallization in a ‘trapped magma’ environment and gives a similar trend, but to a greater degree of evolution, than that of the cumulus loparite. The parent magma of the Lovozero intrusion, Phases II and III, was initially

undersaturated with respect to loparite and only after the crystallization of about 30% of the original melt did loparite appear as a cumulus phase (together with nepheline, microcline, clinopyroxene and amphibole), and accumulate to form the loparite ores. The principal processes involved were probably a combination of magmatic convection coupled with settling of loparite at the base of units of urtite, foyaite and lujavrite. Each unit consists of three seams enriched in nepheline + loparite, followed by nepheline + feldspar, and finally nepheline + feldspar + aegirine.

The partition coefficients of REE, Sr, Nb and Th between loparite and melt are relatively constant and independent of temperature and melt composition, which is in good agreement with the experimental data (*Kogarko* et al., 1983).

During the evolution of the peralkaline nepheline syenite magma there was enrichment of alkalis and volatiles in the residual melt. Loparite became unstable during the post-cumulate stage and was replaced by a range of minerals including barytolamprophyllite, lomonosovite, steenstrupine-(Ce), vuonnemite, nordite, nenadkevichite, REE, Sr-rich apatite, vitusite-(Ce), mosandrite, monazite-(Ce), cerite and Ba, Si-rich belovite.

## Acknowledgements

Various versions of this manuscript have been significantly improved as a result of constructive comments from *M. Henderson*, *M. Le Bas*, *A. Rukhlov*, *H. Sørenson*, two anonymous reviewers, and editorial comments from *A. Finch*. We are grateful to The Royal Society for a grant which enabled *LNK* to undertake analytical work at the Natural History Museum, London, and for all three authors to collect material from Lovozero. For assistance in the field, and other logistical help, we thank *A. Arzamastsev*. This work was also partly supported by a RFBR Grant No. 99-05-64835, and NATO Grant No. 97-5118.

## References

*Arzamastsev AA, Arzamastseva LV, Glasnev VN, Raevsky AB* (1998) Deep structure and the composition of deep parts of Khibina and Lovozero complexes, Kola Peninsula, petrological and geophysical model. J Petrol 6: 478–496

*Balashov YuA, Turanskaya NV* (1960) Regularities in the distribution of rare-earth elements in rocks of the Differentiated complex of the Lovozero alkaline massif in connection with some problems of the genesis of this complex (in Russian). Geokhimiya 701–713

*Clark AM* (1993) Hey's mineral index. Chapman and Hall, London, 844 pp

*Eliseev NA, Fedorov EE* (1953) Lovozero pluton and its mineral deposits. Trans Laboratory Geol of the Precambrian, St Petersburg, 307 pp

*Gerasimovsky VI, Kostyleva EE* (1937) Loparite minerals of Khibina and Lovozero tundras (in Russian). Acad Sci, St Petersburg, pp 408–419

*Gerasimovsky VI, Volkov VP, Kogarko LN, Polyakov AI, Saprykina TV, Balashov YuA* (1966) The geochemistry of the Lovozero alkaline massif, part 1. Geology and Petrology. Part 2. Geochemistry. Translated 1968 by *Brown DA*. Australian National University Press, Canberra, 224 and 369 pp (Translation of original Russian text published in 1966)

*Henderson P* (1975) Geochemical indicator of the efficiency of fractionation of the Skaergaard Intrusion, East Greenland. Min Mag 40: 286–291

*Hunter RH* (1996) Texture development in cumulate rocks. In: *Cawthorn RG* (ed) Layered intrusions. Elsevier, Amsterdam, pp 77–101 (Dev Petrol 15)

*Ifantopulo TN, Osokin ED* (1979) Accessory loparite from stratified alkaline intrusions (in Russian). In: New data on mineralogy of mineral deposits from alkaline rocks. Trans Institute Mineral Geochem and Crystallog Rare Elements, NEDRA, pp 20–28

*Khomyakov AP* (1995) Mineralogy of hyperagpaitic alkaline rocks. Clarendon Press, Oxford, 223 pp

*Kogarko LN* (1977) Genetic problems of agpaitic magmas (in Russian). Nauka, Moscow, 294 pp

*Kogarko LN* (1990) Ore-forming potential of alkaline magmas. Lithos 26: 165–175

*Kogarko LN, Volkov VP* (1963) Physical-chemical evolution of differentiated complex of Lovozero massif in connection with its layering (in Russian). In: Chemistry of the Earth's Crust 1. Nauka, Moscow, pp 111–127

*Kogarko LN, Khopaev V* (1987) The modelling of formation of apatite deposits of the Khibina massif (Kola Peninsula). In: *Parsons I* (ed) Origin of igneous layering. Reidel Publishing Company, Dordrecht, pp 589–611

*Kogarko LN, Ryabchikov ID, Sørensen H* (1974) Liquid fractionation. In: *Sörensen H* (ed) The alkaline rocks. John Wiley, London, pp 488–500

*Kogarko LN, Burnham CW, Shettle D* (1977) The water regime in hyperalkaline magmas. Geochem Int 14: 1–9

*Kogarko LN, Veksler IV, Krigman LD* (1983) Magmatic crystallization of loparite in the system loparite-nepheline. Dokl Acad Sci USSR, Earth Sci Sect 268: 1213–1215

*Kogarko LN, Kononova VA, Orlova MP, Woolley AR* (1995) Alkaline rocks and carbonatites of the world, part 2. Former USSR. Chapman and Hall, London, 226 pp

*Kogarko LN, Williams T, Osokin ED* (1996) The evolution of loparite compositions in the Lovozero massif. Geochem Int 34: 262–265

*Kramm U, Kogarko LN* (1994) Nd and Sr isotope signatures of the Khibina and Lovozero agpaitic centres, Kola alkaline province, Russia. Lithos 32: 225–242

*Kravchenko SM, Saytsev YeI, Shatagina YeV* (1974) Uranium as an indicator of magmatic processes of formation of differentiated intrusives (with Lovozero pluton as an example). Dokl Acad Sci USSR Earth Sci Sect 218: 215–218

*Le Maitre RW* (1989) A classification of igneous rocks and glossary of terms. Blackwell Scientific Publications, Oxford, 193 pp

*Mandarino JA* (1999) Fleischer's glossary of mineral species. The Mineralogical Record Inc, Tuscon, 225 pp

*Marsh BD, Maxey MR* (1985) On the distribution and separation of crystals in convecting magma. J Volcanol Geotherm Res 24: 95–150

*Mitchell RH* (1996) Perovskites: a revised classification scheme for an important rare earth element host in alkaline rocks. In: *Jones AP, Wall F, Williams CT* (eds) Rare earth minerals: chemistry, origin and ore deposits. Chapman and Hall, London, pp 41–76 (Mineral Soc Series 7)

*Mitchell RH, Chakhmouradian AR* (1996) Compositional variation of loparite from the Lovozero alkaline complex, Russia. Can Mineral 34: 977–990

*Naslund HR, McBirney AR* (1996) Mechanisms of formation of igneous layering. In: *Cawthorn RG* (ed) Layered intrusions. Elsevier, Amsterdam, pp 1–43 (Dev Petrol 15)

*Parsons I* (1987) Origins of igneous layering. Reidel Publishing Company, Dordrecht, 531 pp

*Ramsay W, Hackman V* (1894) Das Nephelinsyenitgebiet auf der Halbinsel Kola, I. Fennia (in German). Bull Soc Geogr Finlande (Helsingfors) 11 (2): 1–225

*Shablinskiy GN* (1963) On the minor structure of the Khibina and Lovozero plutons (in Russian). Trans Leningrad Nat Hist Soc 74: 41–43

*Smirnov VI* (1976) Rare earth deposits (in Russian). In: Geology of mineral deposits. NEDRA, Moscow, pp 116–119

*Sparks RSJ, Huppert HE, Koyaguchi T, Hallworth MA* (1993) Origin of modal and rhythmic igneous layering by sedimentation in a convecting magma chamber. Nature 361: 246–249

*Veksler IV, Kogarko LN, Krigman LD* (1984) Phase equilibria in the loparite-nepheline system. Geochem Int 21: 145–150

*Veksler IV, Kogarko LN, Krigman LD, Senin VG* (1989) Loparite crystallization from lujavrite under dry and saturated conditions. Geochem Int 26: 15–24

*Vlasov KA, Kuz'menko MV, Es'kova EM* (1966) The Lovozero alkali massif. Oliver and Boyd, Edinburgh, 627 pp (first published 1959 by Akademii Nauk SSSR, Moscow)

*Vorob'eva OA* (1938) On the genesis of the loparite deposits of the Lovozero massif (in Russian). Izvestia Akad Sci USSR Geol Ser 3

*Williams CT* (1996) Analysis of rare earth minerals. In: *Jones AP, Wall F, Williams CT* (eds) Rare earth minerals: chemistry, origin and ore deposits. Chapman and Hall, London, pp 327–348 (Mineral Soc Series 7)

*Wörner G, Beusen J-M, Duchateau N, Gijbels R, Schminke H-U* (1983) Trace element abundances and mineral/melt distribution coefficients in phonolites from the Laacher See volcano (Germany). Contrib Mineral Petrol 84: 152–173

Authors' addresses: *L. N. Kogarko*, Vernadsky Institute, Kosygin Street 19, Moscow 117975, Russia; *C.T. Williams* (corresponding author), e-mail: t.williams@nhm.ac.uk, and *A.R. Woolley*, Department of Mineralogy, Natural History Museum, Cromwell Road, London SW7 5BD, United Kingdom.